

Influence of the ratio of group III and V fluxes on the structural, emissive properties and stimulated emission of planar structures with InGaN layers in the IR range

© D.N. Lobanov¹, M.A. Kalinnikov¹, K.E. Kudryavtsev¹, B.A. Andreev¹, P.A. Yunin¹,
A.V. Novikov¹, E.V. Skorokhodov¹, Z.F. Krasilnik^{1,2}

¹ Institute of Physics of Microstructures, Russian Academy of Sciences,
603950 Nizhny Novgorod, Russia

² Lobachevsky State University,
603950 Nizhny Novgorod, Russia

E-mail: dima@ipmras.ru

Received April 15, 2024

Revised June 20, 2024

Accepted June 20, 2024

The influence of the ratio of fluxes of elements of groups III and V on the formation features, structural, emissive properties, as well as the possibility of obtaining stimulated emission in the IR range in planar structures with InGaN layers with an In content of $\sim 50\text{--}100\%$ has been studied. It was found that at a growth temperature of 470°C , in order to obtain InGaN layers of homogeneous composition, the III/V flow ratio must be reduced compared to the stoichiometric ($\text{III/V} < 1$) in order to suppress the processes of thermal decomposition and phase separation. The critical III/V value required to obtain homogeneous InGaN solutions depends non-monotonically on the composition. As the In content decreases to $\sim 80\%$, this ratio increases from 0.75 to 0.85, which is due to the stabilization of the InGaN solution, since the Ga-N atom bonds are stronger than the In-N bonds. With a further decrease in the In content to $\sim 50\%$, the III/V ratio must be reduced to suppress the processes of thermal decomposition and phase separation. The optimal III/V ratio, from the point of view of the lowest stimulated emission thresholds, is close to the critical III/V ratio for obtaining homogeneous InGaN of a given composition. At III/V values greater than critical, processes of thermal decomposition and phase separation are observed in InGaN solutions, and stimulated emission is not observed in such structures. If the III/V ratio decreases significantly below the critical value, as a result of the development of surface roughness and an increase in optical losses, the stimulated emission thresholds significantly increase.

Keywords: InGaN, molecular beam epitaxy, thermal decomposition, spinodal decomposition, stimulated emission of radiation.

DOI: 10.61011/SC.2024.04.58850.6357H

1. Introduction

Group III metal nitrides (AlN, GaN, InN) and their ternary solutions are the base material for effective optoelectronic devices in the ultraviolet (GaN/AlGaIn) and blue-green (GaN/InGaIn) spectral regions [1–3]. The quantum efficiency of InGaIn-based optoelectronic devices rapidly decreases with an increase of the operating wavelength, which is associated with a deterioration of the crystalline quality of the structure with an increase of the In content in InGaIn. This has led to the lack of commercial light sources based on this material in the red and IR ranges [4]. The main problems here are: high dislocation density, the presence of phase decay, the need to reduce the epitaxy temperature (due to low decomposition temperatures $\sim 500^\circ\text{C}$ of InN) and the enhancement of the quantum-dimensional Stark effect [1–7].

Due to the problems outlined above, the authors of this paper has demonstrated only recently the stimulated radiation (SR) from InGaIn planar layers with a content of In $\geq 75\%$ in the near IR range at wavelengths of $1.1\text{--}1.65\ \mu\text{m}$ [8]. Samples with InGaIn layers with In content of $\sim 80\text{--}90\%$ had the lowest excitation threshold,

which is associated with lower Auger recombination coefficients compared to InN. At the same time, an increase of the Ga content in InGaIn to 25% resulted in a sharp increase of the threshold, which was associated with a general deterioration of the crystalline quality of InGaIn as it progressed to solutions of „medium“ compositions, which was associated with an intensification of the processes of phase decay and decomposition. The authors of this paper showed that it is possible to suppress decomposition and phase decay in InGaIn layers of „medium“ compositions (50–60%) by lowering the growth temperature (to $\sim 380^\circ\text{C}$), however, this results in a significant degradation of the crystalline quality and the radiative properties of InGaIn [9]. However, it is possible to obtain homogeneous solutions of InGaIn of „medium“ compositions even at sufficiently high growth temperatures ($\sim 470^\circ\text{C}$) by increasing the flow of the nitrogen component (or lowering the flow ratio III/V), which results in the suppression of decomposition and phase decay processes while maintaining effective interband luminescence [9,10].

This paper presents the results of a study of the ratio of flows of elements groups III and V (III/V) for the possibility of formation of homogeneous InGaIn layers in a wide range

of compositions with In content of 50–100% obtained by plasma-assisted molecular beam epitaxy (PA-MBE) at a fixed high growth temperature ($\sim 470^\circ\text{C}$). The impact of growth stoichiometry on the achievability of stimulated radiation in InGaN layers of these compositions was studied.

2. Experiment procedure

The studied InGaN layers were grown on 2-inch sapphire substrates ($c\text{-Al}_2\text{O}_3$) by the PA-MBE method using STE 3N3 facility (AO „NTO“). High-temperature buffer layers of AlN (200 nm) and GaN (700 nm) were sequentially grown on a sapphire substrate at temperatures (T_{gr}) of 820 and 710°C, respectively. Next, the InGaN layer (~ 700 nm) with In content of 50–100% was grown at a much lower temperature of $T_{gr} \sim 470^\circ\text{C}$. This growth temperature ensured a good crystalline quality and an intense photoluminescence signal at room temperature for InGaN layers of different compositions [8–10].

A thin InGaN layer (~ 15 nm) was formed by metal modulation epitaxy (MME) at 430°C at the initial stage of growth of the InGaN active layer for reducing the density of mismatch dislocations arising from the difference in the parameters of the InGaN lattices and the GaN buffer layer [11]. The In and Ga flows turned on and off simultaneously with the growth of the MME and did not change with the growth of the main InGaN layer. Therefore, the average InGaN composition remained unchanged. Since the total amount of accumulated metal in the phase of metal-enriched MME growth did not exceed 2 ML, InN/InGaN superlattice was not formed during MME growth, which was confirmed by X-ray diffraction analysis [11]. The total rate of metal deposition (In+Ga) during the deposition of the InGaN base layer for all samples remained unchanged and amounted to 0.3–0.35 $\mu\text{m/h}$. Plasma source RF Atom Source HD 25 (Oxford Applied Research) was used to create a stream of activated nitrogen; the nitrogen flow during growth remained unchanged at 2 sccm (standard cubic centimeters per minute), the discharge power of the nitrogen plasma source varied in the range 160–200 W, ensuring a ratio of III/V ~ 0.6 –0.9.

The grown samples were analyzed by X-ray diffraction (XRD), scanning electron microscopy (SEM), photoluminescent (PL) spectroscopy and Hall effect measurements.

The dislocation density was determined by the half-width of diffraction peaks recorded during scanning in the directions (0004) and (10 $\bar{1}$ 2), in accordance with the method described in Ref. [12], and the electron concentration was determined using the Hall effect measurement data.

The samples were excited for PL measurements by a continuous wave laser (CW) operating at a wavelength of 650 nm. The spectrum was recorded using Action 2300i lattice spectrometer with an InGaAs diode matrix (OMA-V, Princeton Instruments) cooled with liquid nitrogen. The stimulated radiation mode was realized with an excitation by a pulsed optical parametric generator, tunable in the range of $\lambda = 0.45$ –2.3 μm , with a pumping power density up to 300 kW/cm² at a pulse duration of 10 ns and a repetition frequency of 10 Hz.

The main parameters of the studied structures with InGaN layers. The proportion of indium (x_{in}) in the composition of the ternary solution, the ratio of element flows (III/V) during growth, dislocation density (N_D), background electron concentration (n_e) and threshold (P_{th}) of transition to stimulated emission (if available) for temperature $T = 77$ K are indicated

Number of sample	x_{in} , %	III/V	N_D , 10^{-10} cm ⁻²	n_e , 10^{19} cm ⁻³	P_{th} , kW/cm ²
1	53	0.65	24	1.9	–
2	67	0.88	7.3	2	–
3	52	0.88	20	1.2	–
4	62	0.64	5.9	1.7	110
5	61	0.74	6.2	1.6	–
6	72	0.71	6.1	1.9	35
7	70	0.67	4.9	1.7	20
8	68	0.65	5	1.5	90
9	70	0.62	5.4	1.6	90
10	65	0.83	12	2	–
11	82	0.69	3.2	1.7	5.2
12	78	0.6	4.5	1.8	55
13	57	0.7	12	1.2	–
14	90	0.75	4.2	1.9	40
15	100	0.65	2.9	1.4	60

3. Results and discussion

The X-ray diffraction method in which the form of the swing curve $\omega - 2\theta$ of reflection (0004) was analyzed played the main role in the study of the homogeneity of the InGaN layers obtained, the establishment of signs of thermal decomposition or phase decay of the deposited layer in them. The homogeneity (symmetry) of the main InGaN peak and the presence of a response corresponding to InN were evaluated. The typically measured XRD spectra of structures with an active InGaN layer are shown in Figure 1, *a* to illustrate the approach used (the curve numbers correspond to the sample numbers in the table).

Here, the curve 1 (with a symmetrical peak of InGaN reflection) corresponds to the formation of a homogeneous InGaN layer, the curve 2 (containing the response of the binary InN) corresponds to the layer with a partial decomposition, and the curve 3 (with signal from InN and with an arm at the main peak from InGaN, indicating the presence of the InGaN phase with a composition other than the main one) corresponds to layers with pronounced phase decay and partial decomposition.

Similarly, a stability diagram of the high-temperature PA-MBE growth of InGaN layers depending on the nominal composition of the layer and the ratio of flows III/V was constructed based on the analysis of the XRD spectra of a set of studied samples. This diagram, shown in Figure 1, *b*, displays the three growth modes indicated above, conditionally separated on the parameter plane by dashed lines, and differing in the role of surface diffusion of adatoms. For instance, the greatest enrichment with the nitrogen component (III/V ~ 0.65 –0.7) contributes to the

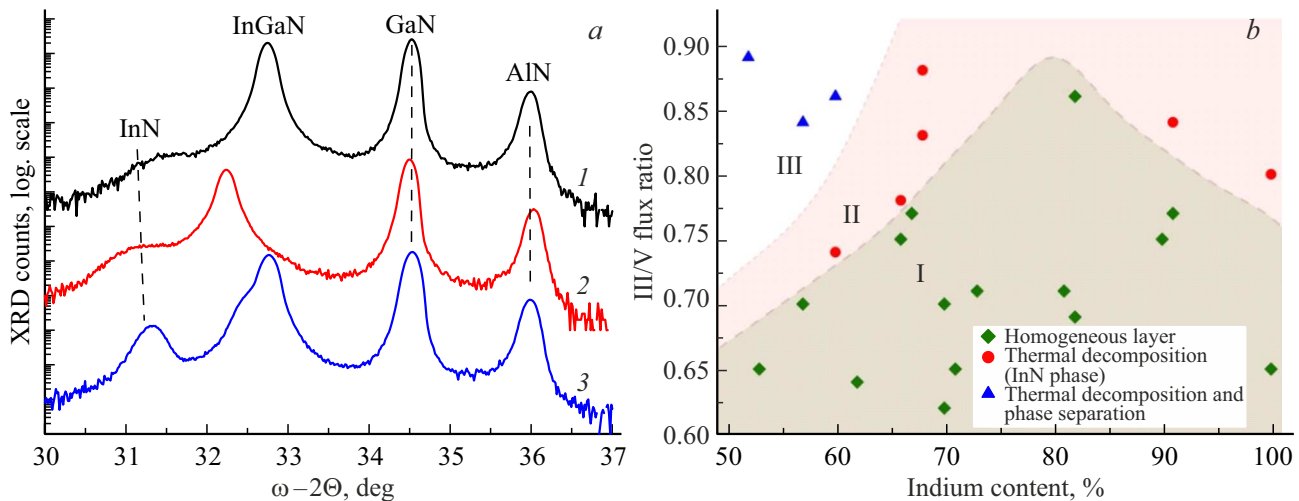


Figure 1. *a* — (0004) $\omega - 2\theta$ X-ray diffraction spectra of samples 1, 2 and 3 from the table. The GaN and AlN reflexes correspond to buffer sublayers. *b* — stability diagram of high-temperature PA-MBE growth of InGaN layers depending on the nominal composition of the layer and the ratio of flows III/V. A dashed line (drawn for clarity) separates the parameter area where homogeneous InGaN layers (I) can be obtained from the area where thermal decomposition of the InGaN layer (II) is observed. A double dashed line (drawn for clarity) separates the parameter region where thermal decomposition is observed (II) from the region where thermal decomposition with phase decay is observed (III).

suppression of diffusion processes and the rapid embedding of metal adatoms into the growing layer; a homogeneous layer is formed in this mode (I in Figure 1, *b*) for all tested compositions of the InGaN triple solution. As the flow of the nitrogen component decreases (the ratio of III/V increases), the prevailing incorporation of Ga atoms and desorption of In determine the transition to InGaN growth with the accumulation of indium metal on the growth surface (II in Figure 1, *b*). The InN phase visible in the XRD spectra is formed here at the end of the InGaN layer growth, when the sample is held in a nitrogen plasma stream during cooling [10]. Pronounced fluctuations in the composition and phase decay of the growing layer occur in the case of a further increase of the ratio of III/V and an approximation to metal-enriched growth conditions (III in Figure 1, *b*). Apparently, this regime is ensured by high surface diffusion of metal adatoms due to the formation of the metal bilayer which is well-known from the literature [13,14].

It can be noted that the critical value of the ratio III/V for the beginning of decomposition increases with a decrease of the In content from 100 to 80%, and as it decreases when approaching the „average“ compositions. This suggests that the rate of decomposition of InGaN at the selected growth temperature behaves in a similar way — a lower nitrogen flow than in the case of growth of binary InN or InGaN with In content of $\sim 50\%$ is needed to suppress the decomposition of InGaN solutions with In content of $\sim 80\%$. A similar behavior of the critical temperature of InGaN decomposition from the composition was observed in Ref. [15]. The addition of a small number of Ga atoms (up to $\sim 20\%$) first stabilizes the InGaN solution, since Ga-N bonds are stronger than In-N bonds, which results in an increase of the decomposition temperature of

InGaN. However, the decomposition temperature sharply drops with a further increase of the Ga content, which is associated with intensifying phase decay processes. It is also worth noting that no phase decay is observed in this paper ($\sim 470^\circ\text{C}$) in InGaN layers with a decrease of the In content to $\sim 70\%$ regardless of the ratio of III/V at InGaN growth temperatures. Apparently, the formation conditions for the growth temperatures used are significantly closer to equilibrium compared to „average“ compositions for InGaN solutions with In content of $> 70\%$ and the manifestation of phase decay is not observed even in case of the transition

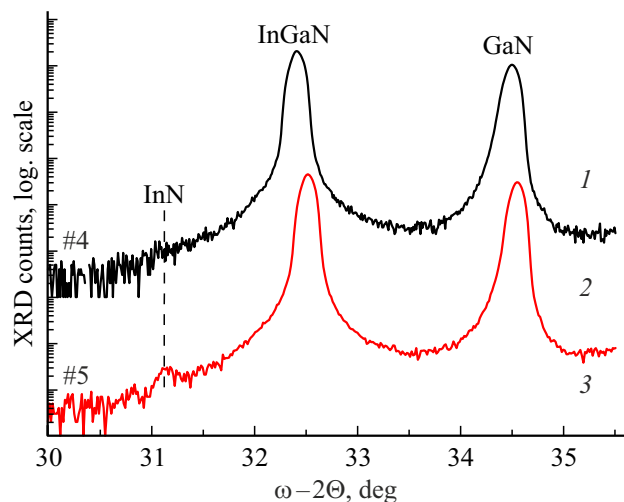


Figure 2. (0004) $\omega - 2\theta$ X-ray diffraction spectra of samples with $\text{In}_{0.6}\text{Ga}_{0.4}\text{N}$ -layers grown with III/V ratio of ~ 0.74 (sample 5, with decomposition) and with III/V ratio of ~ 0.64 (sample 4, homogeneous).

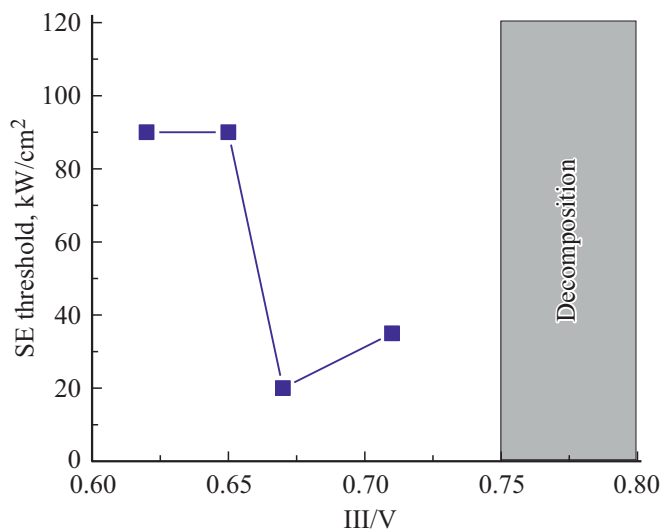


Figure 3. Dependence of the stimulated emission thresholds of samples with InGaN layers, with In content of $\sim 70\%$, on the ratio of III/V (see table, samples 6–9). The gray color indicates the region of parameters of III/V, where decomposition of InGaN layers of this composition is observed and there is no stimulated emission.

to metal-enriched growth conditions. At the same time, InGaN decomposition begins first for the composition range of 50–60%, with an increase of the ratio of III/V flows, and a phase decay is additionally observed with a further increase of III/V.

The discovered structural features of InGaN layers have a significant effect on their optical properties. Figure 2, *a* shows the results of the X-ray diffraction analysis of two samples with InGaN layers with In content of $\sim 60\%$, but with a different III/V ratio of ~ 0.74 and 0.64 (see table, samples 4 and 5). InGaN decomposition is observed in the first case — a weak signal from the binary InN is present in the XRD spectrum, the InGaN layer is homogeneous in the second case. Both samples have a similar density

of threading dislocations and background electron concentration according to the XDA data and measurements of the Hall effect, which indicates a similar level of structural perfection of the samples (see table). However, experiments for the observation of stimulated radiation showed that SR is not observed in a sample with partial decomposition of InGaN, and homogeneous InGaN demonstrates SR with a threshold of $\sim 110 \text{ kW/cm}^2$ at 77 K (see table).

It is assumed that the absence of SR, despite intense PL, in a sample grown in the decomposition conditions is associated with metal-enriched growth conditions, since metal In is present on the surface. As mentioned above, it is its presence when the sample is held in a nitrogen plasma stream during cooling that results in the formation of the InN phase visible in the XRD spectra. Previously, we showed that the growth of InN in metal-enriched conditions results in the formation of deep p-type levels associated with the presence of excess In atoms, which are apparently responsible for rapid recombination by the Shockley–Reed–Hall mechanism, and SR is also not observed in such InN layers [16].

Figure 3 shows the dependence of the observed stimulated radiation thresholds for InGaN samples with In content of $\sim 70\%$ (data from the table for samples 6–9).

SR was observed only in samples with homogeneous InGaN layers (the uncolored area in Figure 3) in experiments aimed at recording stimulated emission, at that time, samples with InGaN obtained in the decomposition conditions did not demonstrate SR regardless of the In content (gray area in Figure 3). The lowest SR thresholds for a fixed InGaN composition were observed at ratios of III/V close to the critical ratios of beginning of decomposition. A further decrease of the ratio of III/V resulted in an increase of the SR observation threshold (Figure 3). The density of threading dislocations weakly depends on the ratio of III/V for homogeneous InGaN layers with In content of $\sim 70\%$ according to the XDA, like the background electron concentration according to the Hall effect data (see table), which indicates a similar level of crystalline quality.

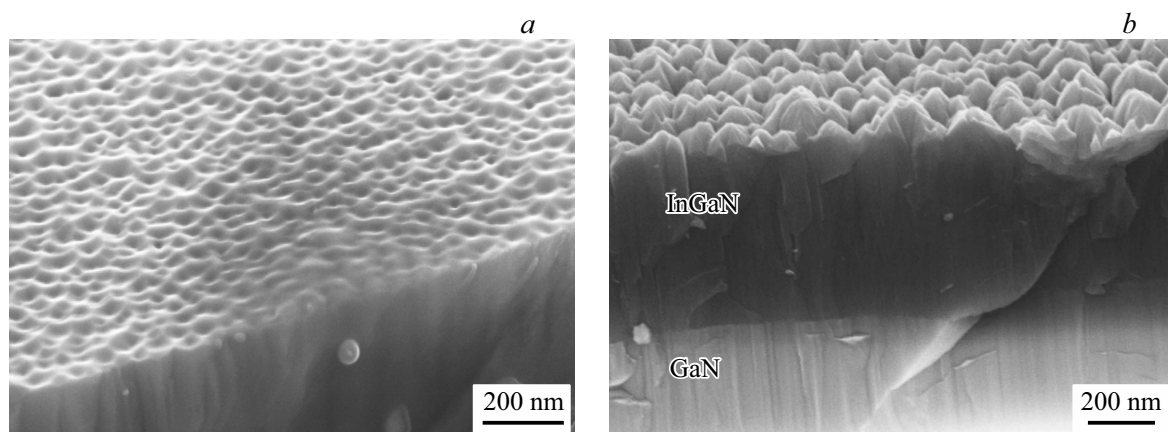


Figure 4. SEM images of the surface of samples 6 and 9 with homogeneous $\text{In}_{0.7}\text{Ga}_{0.3}\text{N}$ -layers grown with a ratio of III/V of ~ 0.71 (*a*) and 0.62 (*b*).

The study of the chips and the surface of structures using SEM methods found that surface roughness develops (Figure 4, *a* and *b*) with a decrease of III/V which is characteristic of the epitaxy of the growth of nitrides of group III by the PA-MBE method [13,14,16].

Previously, we showed that it is the development of surface roughness and the increase of associated optical losses that are responsible for an increase of the SR threshold in InGaN layers with an increase of growth temperature, despite an improvement of crystalline quality and an increase of the photoluminescence signal [17]. Thus, it is the development of surface roughness that is considered the main possible reason resulting in an increase of the SR threshold with a decrease of the III/V ratio in homogeneous InGaN layers.

4. Conclusion

Therefore, this paper studied the possibilities of obtaining by high-temperature PA-MPE growth of high-quality InGaN planar layers with an indium content in the range of 50–100%, which do not demonstrate any signs of thermal decomposition and phase decay. Only such homogeneous structures demonstrate stimulated emission in the IR range, and it is shown that they can be obtained in the entire range of triple solution compositions under consideration due to growth under nitrogen-enriched conditions ($\text{III/V} < 1$). It should be noted that a decrease of the ratio of III/V below the required values results in the development of roughness of the growth surface and an increase of optical losses, which determines the non-monotonic dependence of the SR threshold on the ratio of III/N at a fixed nominal composition of the InGaN active layer, with an optimum near the boundary of thermal decomposition of InGaN.

Funding

The study was performed using the equipment of USU „Femtospekt“ of the Center for Collective Use of the Institute for Physics of Microstructures of the Russian Academy of Sciences with the support of the Russian Science Foundation (RSF grant No. 24-22-00320).

Conflict of interest

The authors declare that they have no conflict of interest.

References

- [1] R. Kour, S. Arya, S. Verma, A. Singh, P. Mahajan, A. Khosla. *ECS J. Solid State Sci. Technol.*, **9**, 015011 (2020). DOI: 10.1149/2.0292001JSS
- [2] Z.C. Feng. *Handbook of Solid-State Lighting and LEDs* (Boca Raton, FL, CRC Press, Taylor & Francis Group, 2017) p. 3. DOI: 10.1201/9781315151595
- [3] F. Roccaforte, M. Leszczynski. *Nitride Semiconductor Technology Power Electronics and Optoelectronic Devices* (Wiley-VCH Verlag GmbH & Co. KGaA, 2020) p. 254.
- [4] B. Damilano, B. Gil. *J. Phys. D: Appl. Phys.*, **48** (40), 403001, (2015). DOI: 10.1088/0022-3727/48/40/403001
- [5] C. Adelman, R. Langer, G. Feuillet, B. Daudin. *Appl. Phys. Lett.*, **75**, 3518 (1999). DOI: /10.1063/1.125374
- [6] G.B. Stringfellow. *J. Cryst. Growth*, **312**, 735 (2010). DOI: 10.1016/j.jcrysgro.2009.12.018
- [7] H. Chen, R.M. Feenstra, J.E. Northrup, T. Zywiets, J. Neugebauer, D.W. Greve, *J. Vac. Sci. Technol. B*, **18**, 2284 (2000). DOI: 10.1116/1.1306296
- [8] D.N. Lobanov, K.E. Kudryavtsev, M.I. Kalinnikov, L.V. Krasilnikova, P.A. Yunin, E.V. Skorokhodov, M.V. Shaleev, A.V. Novikov, B.A. Andreev, Z.F. Krasilnik. *Appl. Phys. Lett.*, **118**, 151902 (2021). DOI: 10.1063/5.0047674
- [9] B.A. Andreev, D.N. Lobanov, L.V. Krasil'nikova, K.E. Kudryavtsev, A.V. Novikov, P.A. Yunin, M.A. Kalinnikov, E.V. Skorokhodov, Z.F. Krasil'nik. *FTP*, **56** (7), 700 (2022). (in Russian). DOI: 10.21883/FTP.2022.07.52763.18
- [10] M.A. Kalinnikov, D.N. Lobanov, K.E. Kudryavtsev, B.A. Andreev, P.A. Yunin, L.V. Krasilnikova, A.V. Novikov, E.V. Skorokhodov, Z.F. Krasil'nik. *FTP*, **57** (6), 444 (2023). (in Russian). DOI: 10.21883/FTP.2023.06.56472.38k
- [11] B.A. Andreev, D.N. Lobanov, L.V. Krasil'nikova, K.E. Kudryavtsev, A.V. Novikov, P.A. Yunin, M.A. Kalinnikov, E.V. Skorokhodov, M.V. Shaleev, Z.F. Krasil'nik. *FTP*, **55** (9), 766 (2021). (in Russian). DOI: 10.21883/FTP.2021.09.51292.22
- [12] M.A. Moram, M.E. Vickers. *Rep. Progr. Phys.*, **72**, 036502 (2009). DOI: 10.1088/0034-4885/72/3/036502
- [13] E.J. Tarsa, B. Heying, X.H. Wu, P. Fini, S.P. den Baars, J.S. Speck. *J. Appl. Phys.*, **82**, 5472 (1997). DOI: 10.1063/1.365575
- [14] E. Dimakis, E. Iliopoulos, K. Tsagaraki, A. Georgakilas. *Appl. Phys. Lett.*, **86**, 133104 (2005). DOI: 10.1063/1.1891292
- [15] H. Komaki, T. Nakamura, R. Katayama, K. Onabe, M. Ozeki, T. Ikari. *J. Cryst. Growth*, **301**, 473 (2007). DOI: 10.1016/j.jcrysgro.2006.11.123
- [16] B.A. Andreev, D.N. Lobanov, L.V. Krasil'nikova, P.A. Bushuykin, A.N. Yablonskiy, A.V. Novikov, V.Yu. Davydov, P.A. Yunin, M.I. Kalinnikov, E.V. Skorokhodov, Z.F. Krasil'nik. *FTP*, **53** (10), 1395 (2019). (in Russian). DOI: 10.21883/FTP.2019.10.48296.42
- [17] K.E. Kudryavtsev, D.N. Lobanov, L.V. Krasilnikova, A.N. Yablonskiy, P.A. Yunin, E.V. Skorokhodov, M.A. Kalinnikov, A.V. Novikov, B.A. Andreev, Z.F. Krasilnik. *ECS J. Solid State Sci. Technol.*, **11**, 014003 (2022). DOI: 10.1149/2162-8777/ac4d80

Translated by A.Akhtyamov